The International Journal of Advanced Manufacturing Technology
https://doi.org/10.1007/s00170-026-19374-x

ORIGINAL ARTICLE

Thermal management and process efficiency in thin-wall steel wire arc additive manufacturing: a comparison of dwell-time and interpass-temperature control strategies

Lila Bernhardt[1] · **Christopher Saldaña**[1] · **Katherine Fu**[2]

Received: 24 August 2026 / Accepted: 15 October 2026
© The Author(s) 2026

Abstract

Wire arc additive manufacturing (WAAM) enables large-scale metal deposition but is susceptible to thermal accumulation, which can affect geometric consistency and material response. This study experimentally compares fixed dwell-time and interpass-temperature-based thermal management in ER70S-6 steel thin-wall WAAM to evaluate their effects on thermal behavior, geometry, hardness, and production efficiency. Eight fixed dwell times (10–120 s) and five interpass-temperature setpoints (150–500 °C) were investigated using infrared thermography, geometric measurements, and Rockwell B hardness testing. Shorter dwell times and higher interpass temperatures increased thermal accumulation, producing wider, shorter walls and greater hardness variation. Increased cooling improved geometric consistency and hardness uniformity, with the largest changes occurring between approximately 40–60 s dwell and 300–200 °C interpass temperature. Beyond approximately 60 s dwell or below 200 °C, additional cooling produced comparatively smaller improvements while increasing production time. Both strategies limited thermal accumulation when sufficient cooling was provided, but temperature-based deposition adjusted dwell duration according to the measured thermal state rather than imposing a fixed interval. This direct comparison provides process-planning guidance for balancing dimensional consistency, hardness response, and production efficiency. The identified operating region is specific to the investigated material, geometry, and deposition conditions.

Highlights

- Compares dwell-time and interpass-temperature control in WAAM.
- Infrared monitoring links thermal history to geometry and hardness.
- Thermal accumulation increases width and hardness variability.
- Benefits diminish beyond 60 s dwell or 200 °C under tested conditions.
- Temperature-based deposition adjusts cooling time to measured thermal state.

Keywords Wire arc additive manufacturing (WAAM) · Interpass temperature control · Dwell time · Thermal management · Geometric stability · Process efficiency

✉ Katherine Fu
kfu26@wisc.edu

Lila Bernhardt
lbernhardt7@gatech.edu

Christopher Saldaña
christopher.saldana@me.gatech.edu

[1] School of Mechanical Engineering, Georgia Institute of Technology, Atlanta, GA, USA

[2] Department of Mechanical Engineering, University of Wisconsin-Madison, Madison, WI, USA

1 Introduction

Wire arc additive manufacturing (WAAM) is a large-scale metal additive manufacturing process that offers high deposition rates and compatibility with conventional welding and CNC platforms, making it attractive for cost-effective fabrication of near-net-shape metallic structures [1–4]. However, thermal accumulation during multilayer deposition can lead to excessive bead width, reduced build height, geometric deviations, and changes in local material response [5–8].

Published online: 20 October 2026

Effective management of heat input and inter-layer cooling is therefore important for maintaining dimensional consistency and material properties while preserving the productivity advantages of WAAM.

Thermal accumulation affects bead morphology and dimensional stability as successive layers are deposited. Increasing build height can reduce cooling rates and increase interpass temperatures, promoting bead spreading and reduced vertical buildup [5–7]. Similar thermal behavior has been observed in carbon and stainless steel WAAM systems [9–11]. In low-carbon-steel WAAM, thermal history and build position have also been associated with variations in bead geometry, microstructural evolution, and hardness [12, 13]. Rafieazad et al. [9] and Dirisu et al. [14] documented layer-dependent variations in microstructure and hardness, while Ge et al. [15] demonstrated that inter-layer dwell duration influences microstructural evolution through its effects on cooling rate and thermal history. These findings establish the importance of controlling thermal accumulation to improve geometric consistency and local material response.

1.1 Inter-layer thermal management strategies

Two commonly used approaches to managing inter-layer thermal conditions are fixed dwell time and interpass-temperature-based deposition. Fixed dwell schedules impose a prescribed cooling interval between successive layers and are relatively straightforward to implement without additional thermal feedback [5, 16, 17]. However, because heat-dissipation conditions change as the wall grows, a fixed cooling interval may permit progressively increasing interpass temperatures and geometric variation [9, 18]. Nagasai et al. [17] demonstrated that extending dwell duration can improve bead geometry, although the benefits diminish as cooling time increases.

Interpass-temperature-based deposition instead uses thermal measurements to determine when the next layer should begin, allowing the cooling interval to respond to the evolving thermal state of the deposited material [19]. This approach accounts for changes in the thermal state of the deposited material rather than imposing a constant cooling interval. Aldalur et al. [19] investigated the effects of interpass-temperature constraints on mild-steel WAAM, while Ma et al. [20] and Hackenhaar et al. [21] demonstrated that thermal targeting and auxiliary cooling can improve process stability. Scotti et al. [22] also investigated the effects of controlled metal transfer and cooling on thermal behavior in steel WAAM. More recently, Carvalho and Campatelli [23] demonstrated that interpass-temperature control influences geometric uniformity and mechanical response in Ti-6Al-4 V WAAM, highlighting the importance of balancing cooling conditions, material response, and productivity. Although the specific thermal response and resulting material properties depend on the alloy and deposition conditions, these studies demonstrate the broader importance of inter-layer thermal management.

1.2 Thermal management and manufacturing efficiency

Thermal management also introduces a trade-off between part consistency and manufacturing efficiency. Increasing cooling duration can reduce thermal accumulation and improve geometric stability but adds nonproductive time to the deposition process. Suryakumar et al. [24] emphasized the contribution of inter-layer dwell to total build time, while Thien et al. [25] quantified the effects of process parameters on steel WAAM productivity. Active cooling approaches, including forced convection and directed gas cooling, have also been investigated to improve thermal stability while reducing cooling-related idle time [20, 21]. These studies demonstrate that selecting thermal-management parameters requires consideration of both the resulting part characteristics and the production time required to achieve them.

1.3 Research gap and study objectives

Although previous studies have established the effects of dwell duration, interpass temperature, and auxiliary cooling on WAAM performance, direct experimental comparisons of fixed dwell-time and interpass-temperature-based deposition under common processing conditions remain relatively limited. In particular, the combined effects of these two strategies on thermal accumulation, wall geometry, hardness distribution, and production time have not been extensively quantified for ER70S-6 mild-steel thin walls. This distinction is important for process planning because fixed dwell schedules prescribe cooling time, whereas temperature-based deposition adjusts the cooling duration according to the measured thermal state. Understanding the relative performance of these approaches can help determine when additional cooling provides meaningful improvements in part consistency and when the associated increase in production time outweighs those benefits.

This study addresses this gap through a direct experimental comparison of fixed dwell-time and interpass-temperature-based thermal management in ER70S-6 mild-steel thin-wall WAAM. Walls were fabricated using dwell times ranging from 10 to 120 s and interpass-temperature setpoints ranging from 500 to 150 °C. In-situ infrared thermography, geometric measurements, Rockwell B hardness testing, and production-time measurements were used to evaluate the effects of the two strategies. Rather than introducing a new

thermal-control method, the contribution is a quantitative comparison of two readily implementable approaches under common processing conditions, with particular emphasis on the trade-offs among thermal stability, geometric consistency, hardness response, and manufacturing efficiency.

The study addresses three research questions:

RQ1 How do fixed inter-layer dwell time and interpass-temperature-based deposition affect wall geometry in thin-wall ER70S-6 WAAM?

RQ2 How do fixed inter-layer dwell time and interpass-temperature-based deposition affect hardness magnitude and distribution across the build height?

RQ3 How are inter-layer cooling conditions, thermal accumulation, wall geometry, hardness, and total production time related, and what trade-offs emerge between process stability and production efficiency?

Based on previous findings concerning thermal accumulation, inter-layer cooling, and material response in WAAM, five hypotheses were formulated:

H1 Depositions with longer inter-layer dwell times and lower interpass temperatures will produce taller, narrower walls and higher hardness than depositions with shorter dwell times and higher interpass temperatures.

H2 Depositions using constant dwell times will exhibit rising interpass temperatures along the build height, particularly at shorter dwell durations.

H3 Depositions using interpass temperature control will produce more uniform wall geometry and hardness profiles than depositions using fixed dwell times, particularly relative to short fixed-dwell conditions.

H4 Hardness will be higher near the substrate and final layers than through the intermediate wall height.

H5 Improvements in geometric consistency and hardness uniformity will diminish as inter-layer cooling increases, such that additional cooling beyond a sufficiently stable thermal condition will provide progressively smaller benefits relative to the associated increase in production time.

Together, these research questions and hypotheses provide a framework for evaluating the effects of the two thermal-management strategies and identifying process-specific trade-offs between part consistency and manufacturing efficiency.

2 Methodology

2.1 WAAM system

Depositions were conducted using a 3-axis Cincinnati Dart CNC machine retrofitted with a Lincoln Electric welding assembly (Fig. 1A). The assembly consisted of an S500 Power Wave Advanced Process Welder, Magnum PRO Robotic 550 Welding Gun, and AutoDrive 4R220 Wire Drive. The welding torch was mounted coincident with the CNC spindle, enabling metal inert gas (MIG) deposition with three degrees of freedom. G-code was used to control the CNC table position and corresponding torch path. A forward-looking infrared (FLIR) A35 camera was mounted to the machine-tool table using a custom aluminum bracket such that the build plate and deposited walls remained stationary within its field of view (Fig. 1B). Welder control and data acquisition were performed using an NVIDIA Jetson Nano and BeagleBone Black. Together, these edge devices facilitated communication among the CNC machine, welder, infrared camera, and a cloud-based monitoring framework comprising a real-time dashboard and SQL database.

The infrared camera was used to monitor relative thermal behavior and interpass temperature evolution throughout the deposition process. According to the manufacturer's specifications, the FLIR A35 has an upper measurement range of 550 °C and a stated accuracy of ± 5 °C or ± 5% of the reading. Temperatures approaching or exceeding 550 °C were therefore interpreted qualitatively as indicators of high thermal accumulation rather than as precise absolute temperature measurements. Thermal measurements were used primarily to compare relative thermal behavior across experimental conditions rather than determine absolute thermodynamic quantities. Similar challenges associated with interlayer temperature measurement and interpretation in thin-wall WAAM have been discussed by Jorge et al. [26].

2.2 Design of experiments

To evaluate the influence of inter-layer thermal-management strategy, two experimental sets were conducted. The first comprised eight fixed-dwell conditions, each represented by a single deposited wall, with dwell times ranging from 10 s to 120 s. Dwell durations were implemented through G-code-controlled pauses between successive layers. The second comprised five interpass-temperature-controlled conditions, each represented by a single deposited wall, with target temperatures ranging from 500 °C to 150 °C. The maximum measured interpass temperature along the wall was monitored in real time using the cloud-based dashboard. Deposition was manually paused after each layer and resumed using the CNC machine human-machine interface

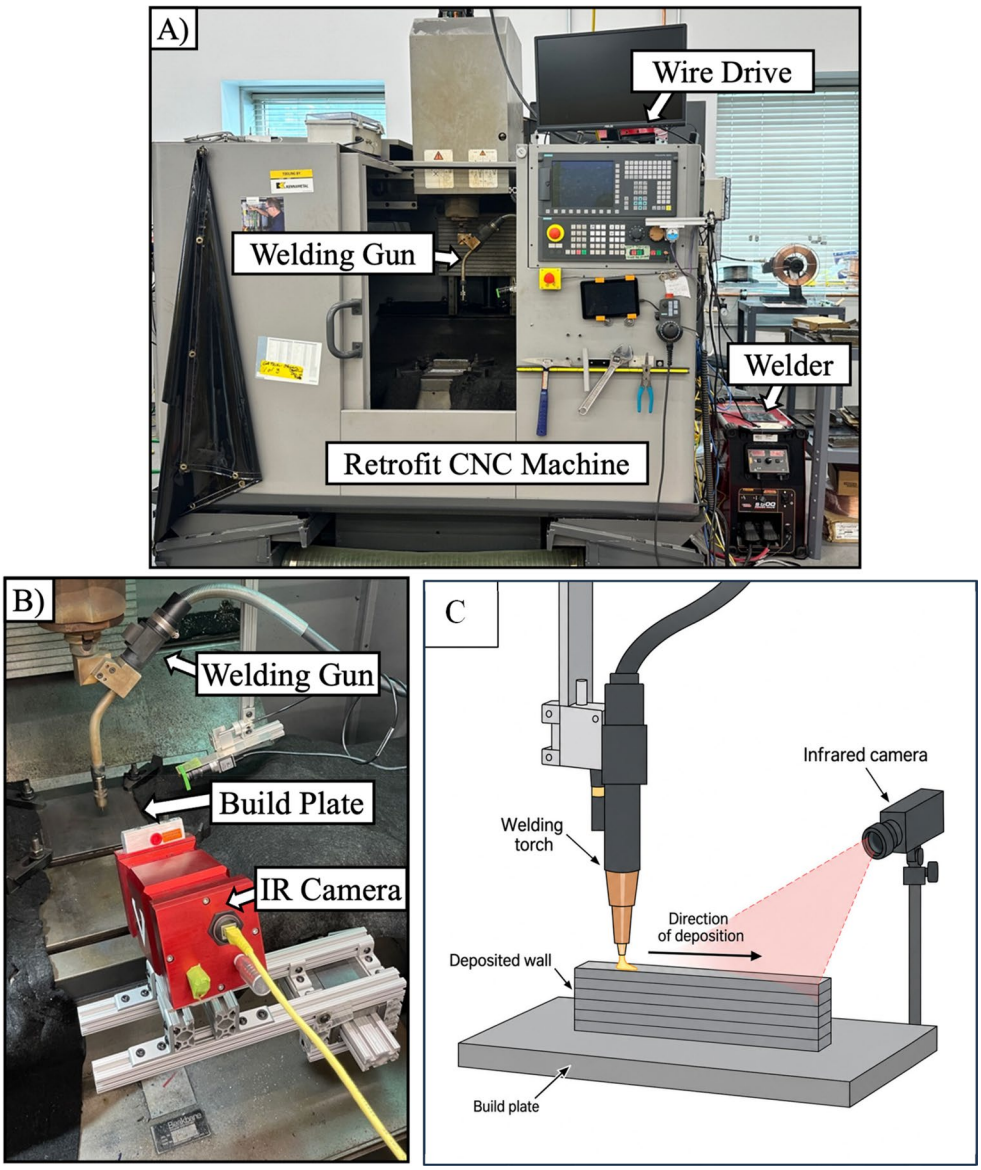


Fig. 1 WAAM experimental setup: (**A**) retrofitted CNC welding assembly, (**B**) infrared camera arrangement, and (**C**) schematic illustration of the welding torch, deposited wall, build plate, infrared camera field of view, and deposition direction

when the measured wall temperature reached approximately the prescribed interpass-temperature setpoint. Thus, the investigated temperature-based strategy represents operator-controlled deposition based on real-time thermal measurements rather than an automated closed-loop control system.

Table 1 summarizes the experimental conditions and corresponding dwell parameters. The fixed-dwell range of 10–120 s and interpass-temperature range of 150–500 °C were selected based on preliminary testing to span conditions exhibiting substantial thermal accumulation through

Table 1 Experimental design sets

Fixed	Target
Dwell Times	Interpass Temps.
10 s	500 °C
20 s	400 °C
30 s	300 °C
40 s	200 °C
60 s	150 °C
80 s	
100 s	
120 s	

conditions exhibiting comparatively stable thermal behavior. The selected ranges also provided overlapping thermal conditions for comparing the two strategies. The intermediate settings were included to characterize how thermal response, wall geometry, hardness, and production time changed as inter-layer cooling increased. The ranges were therefore intended to characterize process behavior under the investigated deposition conditions rather than establish universally applicable operating limits.

2.3 Deposition procedure

ER70S-6 mild-steel wire with a diameter of 1.1 mm was used for all depositions; its nominal chemical composition by weight is provided in Table 2. Samples were deposited onto 6.35-mm-thick hot-rolled steel build plates measuring 203 × 203 mm. Each substrate surface was prepared using acetone and steel wool to remove mill scale and surface contaminants and promote consistent weld penetration. The build plate was clamped to the machine table at each corner to provide consistent fixturing and conductive heat transfer. Shielding gas was 99% argon at a flow rate of 30 cfh. Wire feed speed was 5.3 m/min, traverse speed was 0.4 m/min, input arc power was 2.1 kW, and initial contact-tip-to-work distance was 15.2 mm. These parameters were selected based on preliminary experiments that produced stable thin-wall deposition.

Prior to each deposition, the welding torch was centered over the build plate in the x-direction, and the contact-tip-to-work distance was established using a calibrated gauge block. Each wall consisted of 20 single-bead layers deposited over a length of 152.4 mm. Successive layers were deposited in alternating x-directions. Between layers, the torch retracted in the z-direction for the dwell period specified by the experimental condition and then returned to a position 2.03 mm above the preceding layer for subsequent deposition. Multiple walls were deposited on each substrate to improve experimental throughput while maintaining consistent fixturing. The torch y-position was shifted between walls to provide adequate clearance, and deposition of the next wall did not begin until the baseplate temperature had fallen below 50 °C. A new baseplate was installed when the available deposition area was exhausted, typically after approximately eight walls. All other deposition parameters and procedures were held constant across conditions to enable comparison of the two inter-layer thermal-management strategies.

2.4 Measurement preparation and equipment

After all walls had been deposited, the samples were prepared for geometric measurements and hardness testing. The baseplates were sectioned with a bandsaw to separate each wall, and all walls were then cleaned with a wire brush to remove weld slag and other debris. The overall height and width geometry of each wall sample was measured with calipers. A FARO Laser Line Probe HD, attached to a FARO Edge ScanArm, was then used to scan the wall feature geometry. The FARO ScanArm measurements exhibited non-repeatable stitching errors that prevented reliable determination of absolute wall widths from the reconstructed scans. Consequently, maximum wall dimensions were measured using calipers, while individual scanned side profiles were retained for analysis of geometric variation along wall height. This approach avoided reliance on the alignment of opposing scanned surfaces. After all geometric data was collected, the walls were destructively prepared for hardness testing. Each wall sample was then faced on both sides using a manual mill until visually smooth to create a viable surface for hardness testing.

Hardness Rockwell B testing was performed with a 574 Series Wilson Rockwell Hardness Tester in compliance with ASTM E18-22. Prior to hardness testing, instrument calibration was verified using a reference test block to ensure that measurements were within tolerance. Each wall sample was marked with six vertical sampling paths spaced 25.4 mm apart. Hardness measurements were manually collected incrementally from the bottom to the top of the wall along each sampling path. Because testing was performed manually, the precise vertical spacing and number of measurements varied among sampling paths. Testing locations were selected to avoid overlap between adjacent indentations and edge effects associated with the machined wall boundaries. Erroneous readings resulting from sample instability were documented and excluded, and replacement measurements were collected at adjacent valid locations.

Because hardness testing was performed manually, the precise spatial coordinates of individual indentations were determined after testing using machine vision. A calibrated image of each wall containing a dimensional scale was acquired and processed using threshold-based segmentation to identify valid hardness indentations (Fig. 2A). Centroid locations were extracted for each indentation (Fig. 2B), and pixel coordinates were converted to millimeters using the captured scale. Hardness measurements were collected along six vertical sampling

Table 2 ER70S-6 composition by weight%

Element	C	Si	*P*	S	V	Cr	Mn	Fe	Ni	Cu	Mo
% weight	0.09	0.9	0.007	0.007	0.05	0.05	< 1.60	Bal	0.05	0.2	0.05

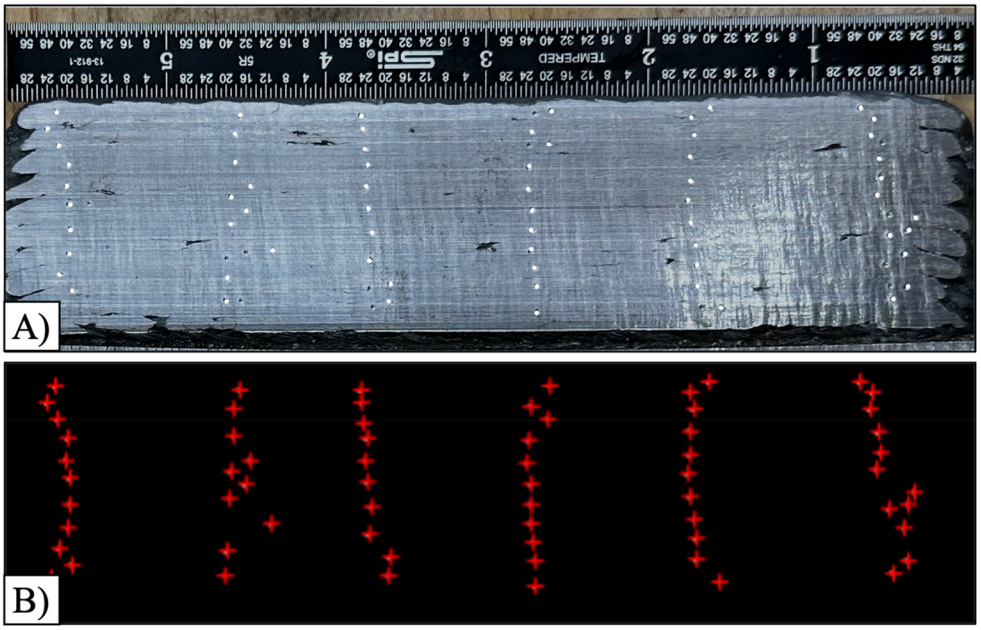


Fig. 2 80 s constant interlayer dwell time sample with (**A**) valid hardness tests highlighted and (**B**) centroid positions located

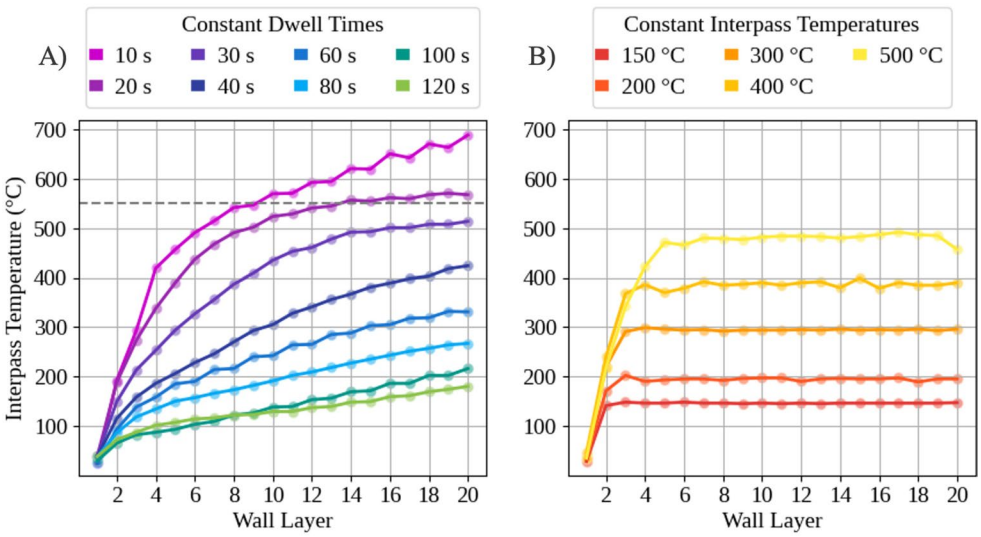


Fig. 3 Interpass temperatures by layer for (**A**) fixed interlayer dwell times and (**B**) interpass-temperature-based deposition. The dashed horizontal line indicates the upper manufacturer-specified measurement limit of 550 °C. Values exceeding this limit are included to illustrate relative thermal accumulation but should not be interpreted as calibrated absolute temperatures

paths distributed across each wall. Measurements along each path were linearly interpolated over wall height to construct continuous hardness profiles. The interpolated profiles were then averaged across the six sampling paths, and measurement heights were normalized by the final wall height to facilitate comparison among experimental conditions.

To quantify geometric variation along wall height, the scanned side profiles were sampled at 1 mm intervals along the wall length and 0.25 mm intervals along the height, excluding the wall endpoints. A reference height of 7.75 mm was used to establish zero relative width deviation. Deviations from this reference were averaged along the wall length and across both side profiles to obtain an average relative width-deviation profile. This approach minimized the influence of alignment errors between the scanned surfaces.

3 Results

3.1 Interpass temperature and cooling behavior

Representative interpass temperature profiles for both strategies are shown in Fig. 3. Under fixed-dwell conditions, interpass temperature increased with build height, with the greatest thermal accumulation observed at shorter dwell durations. The 10 s and 20 s dwell conditions reached or exceeded the manufacturer-specified upper measurement limit of approximately 550 °C within the first 12 layers, indicating substantial thermal accumulation. In contrast, dwell times of 60 s and longer produced comparatively stable interpass-temperature profiles over the remainder of the build.

For the interpass-temperature-controlled conditions, temperatures approached their prescribed setpoints within the initial layers and subsequently remained relatively stable. Mean steady-state interpass temperatures ranged from 4.0 °C below the target for the 150 °C condition to 20.2 °C below the target for the 500 °C condition, with greater deviations observed at higher prescribed temperatures. Achieving lower interpass-temperature setpoints required progressively longer dwell durations between successive layers. The corresponding dwell behavior is shown in Fig. 4. Fixed-dwell builds followed their programmed pauses, while temperature-controlled builds required variable dwell durations to reach the selected temperature, with substantially longer dwell times required at 200 °C and 150 °C.

3.2 Deposition time and process efficiency

Total build time increased with programmed dwell duration across the fixed-dwell conditions, ranging from 11 min 9 s at 10 s dwell to 45 min 57 s at 120 s dwell. For the interpass-temperature-based conditions, cooling durations varied between layers according to the time required to reach the prescribed temperature (Fig. 4). The 200 °C condition required 30 min 10 s, comparable to the 80 s fixed-dwell condition (33 min 18 s), whereas the 150 °C condition required 38 min 41 s, comparable to the 100 s fixed-dwell condition (39 min 37 s). Thus, decreasing the interpass-temperature setpoint from 200 °C to 150 °C increased total deposition time by approximately 28%.

3.3 Geometry outcomes

Dimensional results are summarized in Tables 3 and 4. Shorter fixed dwell times produced wider, shorter walls, while longer dwell times produced narrower, taller walls (Fig. 5). Lower interpass-temperature setpoints were associated with greater wall height, although incomplete width measurements limit assessment of the corresponding width trend.

Across conditions for which both measurements were available, maximum wall height was strongly inversely related to maximum wall width ($R^2 = 0.973$), with wider walls exhibiting correspondingly lower build heights. Geometry variation across wall height is summarized in Fig. 6. Among the fixed-dwell conditions, shorter dwell

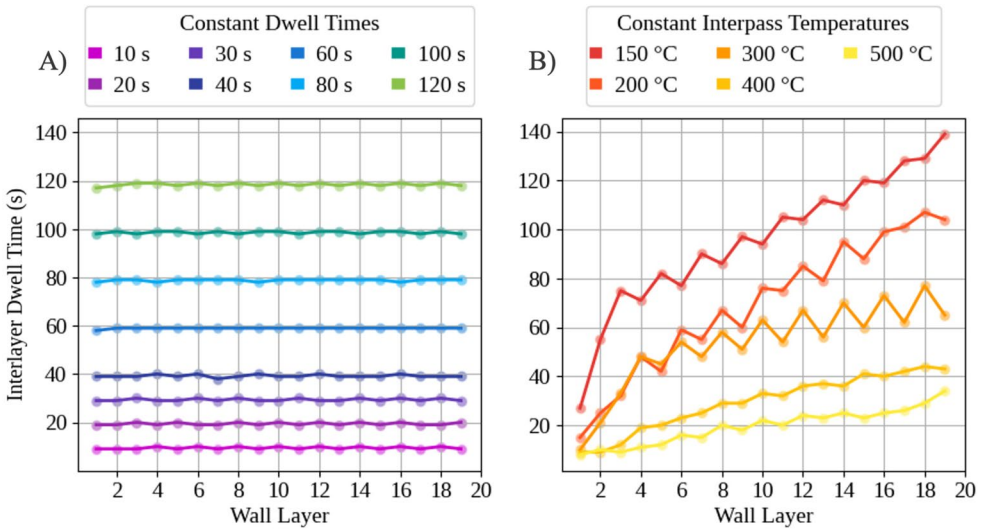


Fig. 4 Interlayer dwell times by layer in depositions with (**A**) constant interlayer dwell times and (**B**) constant interpass temperatures

Table 3 Dimensions of constant interlayer dwell time samples as deposited and after preparation for hardness testing

Interlayer Dwell Time	10 s	20 s	30 s	40 s	60 s	80 s	100 s	120 s
Maximum Width [mm]	9.5	9.3	8.6	7.9	7.8	7.6	7.5	7.4
Maximum Height [mm]	34.2	34.8	36.3	38.4	38.8	40.0	40.1	40.4
Final machined width [mm]	6.2	6.0	6.2	6.3	6.0	6.0	5.8	5.7

Table 4 Dimensions of constant interpass temperature samples as deposited and after preparation for hardness testing

Interpass Temperature	500 °C	400 °C	300 °C	200 °C	150 °C
Maximum Width [mm]	8.5	8.2	8.0	- *	- *
Maximum Height [mm]	36.2	38.0	38.7	40.6	41
Final machined width [mm]	6.3	5.8	6.1	5.8	5.8

Maximum as-deposited width measurements were unavailable for the 200 °C and 150 °C conditions because the scanning errors were identified only after these samples had been destructively prepared for hardness testing

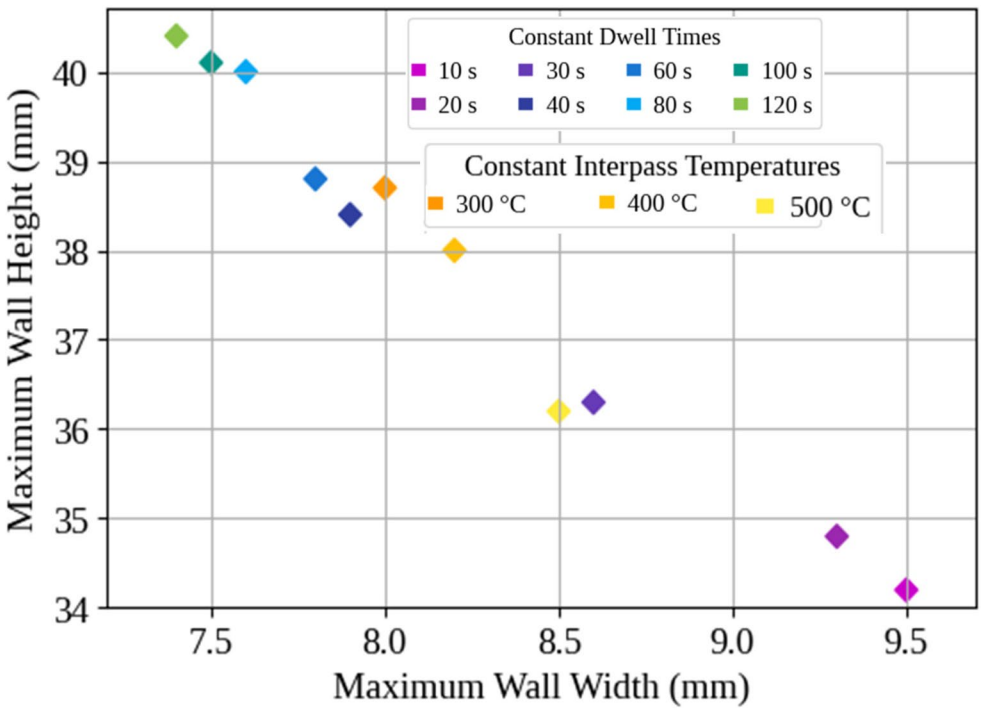


Fig. 5 Maximum wall heights vs. maximum wall widths

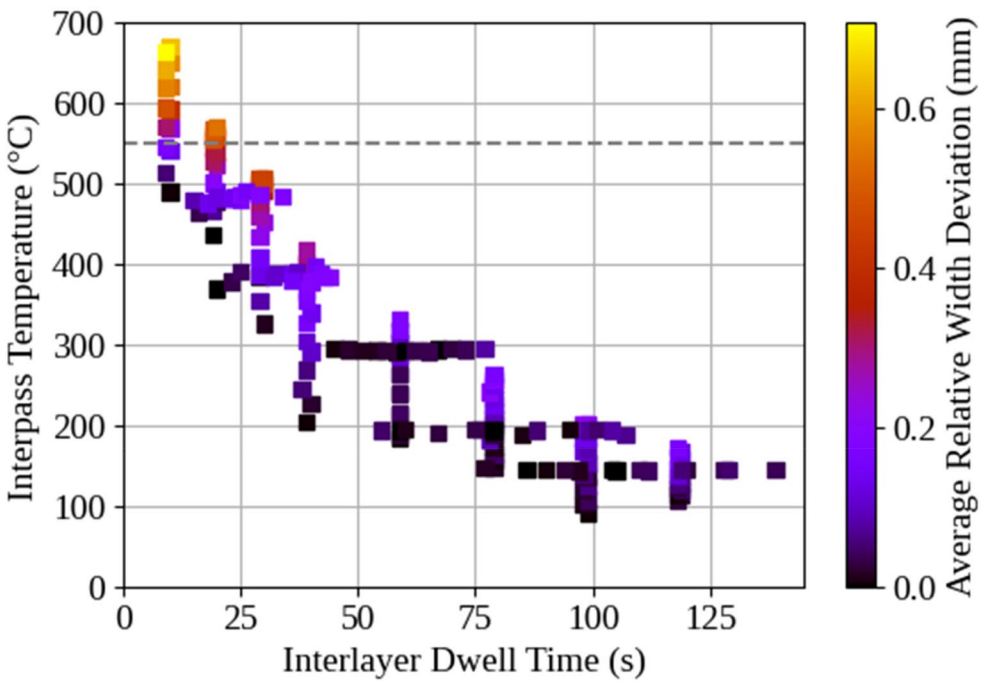


Fig. 6 Average relative width deviation by corresponding interlayer dwell time and interpass temperature pairs

times produced greater width variation, whereas longer dwell times produced more uniform wall profiles.

The interpass-temperature-based conditions also exhibited increasing maximum wall height as the prescribed temperature decreased. However, maximum width measurements were unavailable for the 200 °C and 150 °C conditions, limiting direct comparison of the complete width trend across this experimental set. Among the fixed-dwell conditions, changes in maximum wall dimensions became comparatively small beyond approximately 60 s dwell.

3.4 Hardness profiles

Representative hardness profiles for the fixed-dwell and interpass-temperature-controlled walls are shown in Fig. 7. Across the investigated conditions, hardness was generally

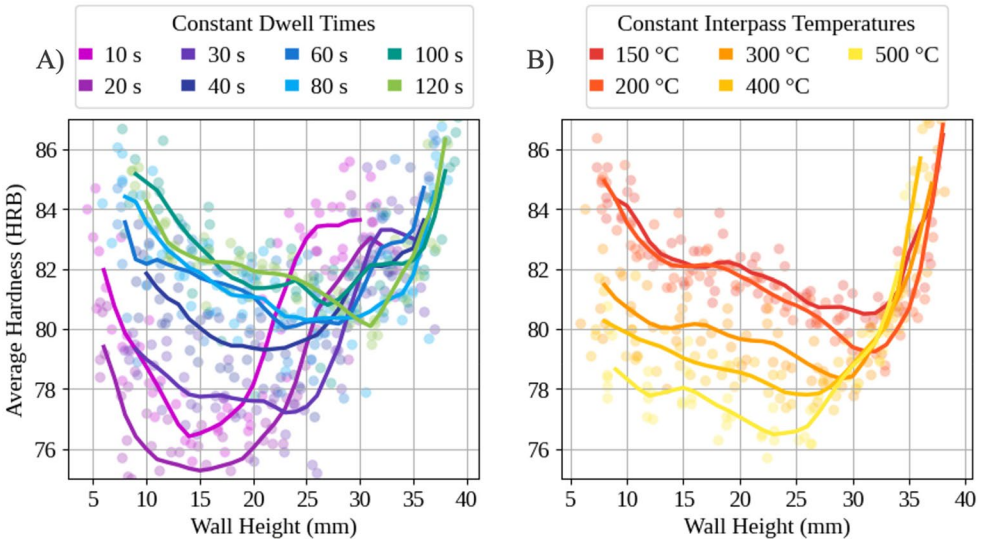


Fig. 7 Average Rockwell B hardness profiles along wall height and hardness measurements in depositions with (**A**) constant interlayer dwell times and (**B**) constant interpass temperatures

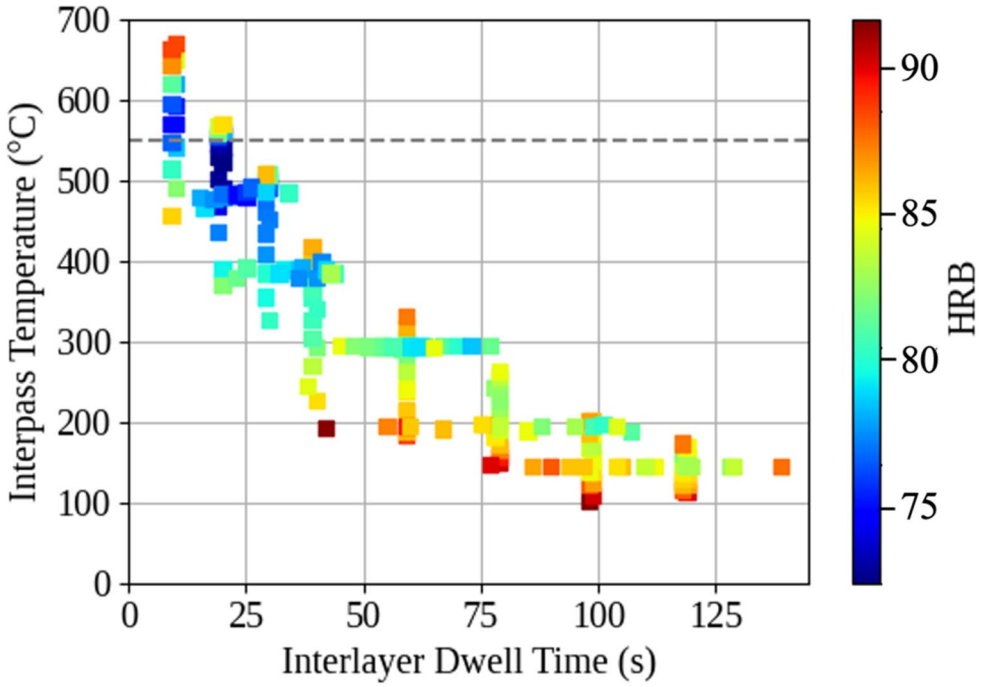


Fig. 8 Rockwell B hardness values by corresponding interlayer dwell time and interpass temperature pairs; color scale represents average Rockwell B hardness, with warmer colors indicating higher hardness values and cooler colors indicating lower hardness values

higher near the substrate and upper wall regions and lower through the intermediate wall height. Longer dwell durations and lower interpass temperatures were associated with higher average hardness and reduced variation across the wall height.

The 10 s dwell condition exhibited greater scatter in hardness than the longer-dwell conditions. The integrated hardness results in Fig. 8 show a general increase in average hardness with increasing cooling duration, with progressively smaller differences among the longer-dwell and lower-interpass-temperature conditions.

3.5 Integrated cooling-geometry-hardness relationships

Figure 8 summarizes the relationship among dwell duration, interpass temperature, and average hardness. Across the thermal, geometric, and hardness results, the largest changes occurred between approximately 40 s and 60 s dwell and between approximately 300 °C and 200 °C interpass temperature. Beyond approximately 60 s dwell or below approximately 200 °C interpass temperature, additional cooling was associated with comparatively smaller changes in the measured outcomes.

These diminishing changes occurred alongside increasing cooling-related production time. For example, increasing fixed dwell time from 60 s to 120 s reduced maximum wall width from 7.8 mm to 7.4 mm, a reduction of approximately 5%, while doubling the programmed inter-layer dwell duration. Together, these results identify an operating region within the investigated process conditions in which additional cooling produced progressively smaller improvements in thermal, geometric, and hardness outcomes relative to the associated increase in production time.

4 Discussion

4.1 Interpass temperature control and geometry uniformity (H1 and H3)

The results are generally consistent with the geometric predictions of H1 and H3. Increasing inter-layer cooling, whether through longer fixed dwell times or lower interpass-temperature setpoints, was associated with greater wall height and improved geometric consistency, while maximum wall width decreased across the measured fixed-dwell conditions. The interpass-temperature-controlled conditions additionally constrained the thermal state at which successive layers were deposited, whereas shorter fixed-dwell conditions exhibited progressive thermal accumulation with build height. These results indicate that the primary advantage of temperature-based deposition is not inherently greater cooling, but the ability to initiate successive layers at a more consistent thermal condition.

The observed geometric trends may be explained by changes in cooling behavior and melt-pool stability during deposition. Higher interpass temperatures can reduce cooling rates and prolong molten-state residence time, potentially promoting lateral material spreading and limiting vertical layer buildup. As thermal accumulation increases through successive layers, the evolving thermal boundary conditions can contribute to increased bead spreading and reduced dimensional consistency.

These trends are consistent with prior studies demonstrating strong relationships among interpass temperature, thermal accumulation, and bead morphology in WAAM [7, 19, 21]. Rafieazad et al. [9] similarly documented changes in material response associated with layer-dependent thermal histories, while prior thermal-management studies have shown that controlling heat accumulation can improve geometric consistency during multilayer deposition [20, 21].

The present results extend this literature by directly comparing fixed-dwell and interpass-temperature-based deposition under common process conditions.

4.2 Role of dwell time and cooling inefficiencies (H2)

The progressive increase in interpass temperature observed under shorter fixed-dwell conditions supports H2. A fixed cooling interval does not account for changes in heat accumulation and dissipation as wall height increases; consequently, shorter dwell durations were insufficient to return the wall to a comparable thermal condition before each successive layer. The resulting relationship between thermal accumulation and wall geometry is consistent with previous thin-wall WAAM studies reporting increased bead spreading under elevated interpass-temperature conditions [19, 27].

Previous studies have demonstrated that active cooling can reduce thermal accumulation while limiting cooling-related idle time [20, 21]. In the present study, increasing fixed dwell duration progressively reduced thermal accumulation, but the associated cooling time increased regardless of whether that duration was required at every layer. In contrast, the interpass-temperature-based approach varied the dwell duration according to the measured thermal state. The comparison therefore highlights a process-efficiency limitation of fixed dwell schedules: a single prescribed interval cannot adapt to changes in cooling demand over the course of the build.

4.3 Hardness trends and microstructural interpretation (H4 and H5)

The observed hardness profiles are consistent with H4, with higher hardness near the substrate and upper wall regions relative to the intermediate wall height. Similar position-dependent hardness distributions have been reported in low-carbon-steel WAAM and attributed to differences in cooling conditions and repeated thermal cycling over the build height [9, 12, 13]. Recent microstructural characterization by Lambiase et al. showed that repeated deposition cycles alter grain morphology and hardness through the build height, while the uppermost layers experience fewer subsequent reheating cycles and exhibit comparatively high microhardness. Because microstructure was not directly characterized in the present study, these mechanisms provide a plausible interpretation of the observed hardness profiles rather than a direct microstructural explanation.

The reduction in hardness variation with increasing cooling duration generally supports H5. Longer fixed dwell times and lower interpass-temperature setpoints were associated with more uniform hardness distributions, while the magnitude of the improvement became comparatively small among the most strongly cooled conditions. Previous studies have similarly demonstrated that cooling conditions

influence thermal history, microstructural evolution, and hardness in steel WAAM [12, 20, 21]. The present results extend this relationship by considering hardness response together with the additional production time required to achieve progressively greater inter-layer cooling.

4.4 Implications for WAAM heat-management strategy

Overall, the results demonstrate that both fixed dwell time and interpass-temperature-based deposition can effectively limit thermal accumulation when sufficient inter-layer cooling is provided. Their principal difference lies in how the cooling requirement is specified. Fixed-dwell schedules impose the same cooling duration after every layer, whereas the temperature-based approach adjusts the duration according to the measured thermal state of the wall. Under the investigated conditions, both strategies produced improved geometric and hardness consistency with increased cooling, although the incremental benefits became smaller as cooling duration increased.

From a process-planning perspective, these results suggest that selection of an inter-layer cooling strategy should consider the incremental improvement in part consistency relative to the additional nonproductive cooling time. Prescribing substantially more cooling than required to reach a comparatively stable thermal regime can increase production time with limited corresponding changes in geometry or hardness. Conversely, insufficient cooling can permit progressive thermal accumulation and associated geometric variation. The appropriate operating condition therefore represents a balance between thermal stability, part consistency, and manufacturing efficiency rather than simply maximizing dwell duration or minimizing interpass temperature.

This interpretation is consistent with recent studies emphasizing similar trade-offs between interpass temperature and productivity. Teixeira et al. [28] demonstrated that cooling strategy and interlayer temperature influence both deposition characteristics and production time, while Carvalho and Campatelli [23] found that additional reductions in interpass temperature produced diminishing geometric and mechanical benefits under their investigated Ti-6Al-4 V conditions. The specific operating regions identified in these studies differ because of material, geometry, heat input, and cooling conditions, reinforcing that such values should be determined for a given process rather than treated as universal thresholds. The present results extend this process-planning perspective to ER70S-6 thin-wall WAAM by directly comparing fixed-time and temperature-based cooling over a common experimental design space.

4.5 Limitations and future work

Several limitations should be considered when interpreting these findings. The study focused on single-bead thin-wall ER70S-6 geometries under a single set of deposition parameters, and each experimental condition was represented by one wall. The results therefore characterize systematic trends across the investigated thermal-management conditions rather than between-build variability or statistically replicated treatment effects. The operating region observed near approximately 60 s dwell and 200 °C interpass temperature should consequently be interpreted as specific to the investigated material, geometry, heat input, and cooling conditions rather than as a universally applicable WAAM process threshold.

Interpass-temperature-based deposition was implemented through manual operator control rather than automated closed-loop control. Although real-time infrared measurements were used to determine when deposition resumed, operator response and measurement uncertainty may introduce variability in the achieved interpass condition. Automated integration of thermal sensing with deposition control would enable more precise evaluation of temperature-based strategies and could permit adaptive adjustment of cooling or process parameters during deposition.

Material response was characterized using Rockwell B hardness only. Tensile strength, toughness, residual stress, and fatigue performance were not evaluated, and hardness uniformity should not be interpreted as demonstrating uniformity in these other mechanical properties. Although the observed hardness trends are consistent with thermal-history effects reported in prior WAAM studies, direct microstructural characterization was not performed. Consequently, the relationships between cooling behavior, microstructural evolution, and hardness discussed here should be interpreted as literature-supported mechanisms rather than experimentally verified transformations. Future work should incorporate metallography, phase characterization, and additional mechanical testing to directly relate thermal history to microstructure and mechanical performance.

Future studies should also extend the comparison to multi-bead and thick-wall geometries, additional steel grades and alloy systems, and a broader range of heat inputs, wire-feed rates, and travel speeds. Automated temperature control combined with predictive thermal models could further enable process-specific cooling conditions to be selected based on desired trade-offs among thermal stability, dimensional consistency, material response, and production efficiency.

5 Conclusion

This study experimentally compared fixed dwell-time and interpass-temperature-based thermal management in ER70S-6 thin-wall WAAM, evaluating thermal accumulation, wall geometry, hardness distribution, and production time. Eight fixed dwell times (10–120 s) and five interpass-temperature setpoints (150–500 °C) were investigated. Shorter dwell times and higher interpass temperatures were associated with greater thermal accumulation, reduced wall height, and increased geometric and hardness variation. Increased inter-layer cooling was generally associated with improved dimensional consistency and hardness uniformity among the tested specimens.

The largest changes in the measured outcomes occurred between approximately 40–60 s dwell and 300–200 °C interpass temperature. Additional cooling beyond approximately 60 s dwell or below 200 °C produced comparatively smaller improvements while increasing production time. For example, increasing fixed dwell time from 60 s to 120 s reduced maximum wall width from 7.8 mm to 7.4 mm, approximately 5%, while doubling the programmed inter-layer cooling interval.

Both strategies limited thermal accumulation when sufficient cooling was provided, but differed in how cooling duration was determined. Fixed-dwell deposition imposed a prescribed interval, whereas temperature-based deposition used measured wall temperature to guide manual resumption of deposition. These findings provide process-planning guidance for balancing geometric consistency, hardness response, and manufacturing efficiency. The identified operating region is specific to the investigated material, wall geometry, and deposition conditions, and requires validation through replicated experiments and additional process configurations.

Acknowledgements This work was funded by the U.S. Department of Energy under award DE-EE-0008303.

Author contributions Lila Bernhardt: methodology, investigation, data curation, formal analysis, visualization, and writing, original draft. Christopher Saldaña: conceptualization, methodology, resources, supervision, and writing, review and editing. Katherine Fu: conceptualization, methodology, supervision, and writing, review and editing. All authors reviewed and approved the final manuscript.

Funding This work was supported by the U.S. Department of Energy through the Enhanced Preparation for Intelligent Cybermanufacturing Systems (EPICS) program under Award No. DE-EE0008303.

Data availability The data supporting the findings of this study are available from the corresponding author upon reasonable request.

Declarations

Ethics Approval Not applicable.

Consent for publication All authors have reviewed and approved the manuscript and consent to its publication.

Consent to Participate Not applicable.

Competing Interests The authors declare no competing interests.

Open Access This article is licensed under a Creative Commons Attribution 4.0 International License, which permits use, sharing, adaptation, distribution and reproduction in any medium or format, as long as you give appropriate credit to the original author(s) and the source, provide a link to the Creative Commons licence, and indicate if changes were made. The images or other third party material in this article are included in the article's Creative Commons licence, unless indicated otherwise in a credit line to the material. If material is not included in the article's Creative Commons licence and your intended use is not permitted by statutory regulation or exceeds the permitted use, you will need to obtain permission directly from the copyright holder. To view a copy of this licence, visit http://creativecommons.org/licenses/by/4.0/.

References

1. Ding D, Pan Z, Cuiuri D, Li H (2015) A review of wire-feed additive manufacturing: technologies, developments and future interests. Int J Adv Manuf Technol 81:465–481
2. Oliveira JP, Santos TG, Miranda RM (2020) Revisiting fundamental welding concepts to improve additive manufacturing: From theory to practice. Prog Mater Sci 107:100590
3. Singh SR, Khanna P (2021) Wire arc additive manufacturing (WAAM): a new process to shape engineering materials. Mater Today: Proc 44:118–128
4. Williams SW, Martina F, Addison AC, Ding J, Pardal G, Colegrove P (2016) Wire + Arc Additive Manuf Mater Sci Technol 32:641–647
5. Kozamernik N, Bračun D, Klobčar D (2020) WAAM system with interpass temperature control and forced cooling for near-net-shape printing of small metal components. Int J Adv Manuf Technol 110:1955–1968
6. Ling Y, Ni J, Antonissen J, Ben Hamouda H, Vande Voorde J, Abdel M, Wahab (2023) Numerical prediction of microstructure and hardness for low carbon steel wire Arc additive manufacturing components. Simul Model Pract Theory 122:102664
7. Yang D, Wang G, Zhang G (2017) Thermal analysis for single-pass multi-layer GMAW based additive manufacturing using infrared thermography. J Mater Process Technol 244:215–224
8. Lambiase F, Yanala PB, Pace F, Andreucci E, Paoletti A (2026) A state of the art review of wire arc additive manufacturing (WAAM) - part2: process improvements and industrial applications. Int J Adv Manuf Technol 143:4623–4654
9. Rafieazad M, Ghaffari M, Vahedi Nemani A, Palmer TA (2019) Microstructural evolution and mechanical properties of a low–carbon low–alloy steel produced by wire arc additive manufacturing. Int J Adv Manuf Technol 105:2121–2134
10. Sridharan N, Noakes MW, Nycz A, Love LJ, Dehoff RR, Babu SS (2018) On the toughness scatter in low alloy C-Mn steel samples

fabricated using wire arc additive manufacturing. Mater Sci Eng A 713:18–27
11. Tenuta E, Nycz A, Noakes M, Simunovic S, Piro MHA (2021) Material properties and mechanical behaviour of functionally graded steel produced by wire-arc additive manufacturing. Addit Manuf 46:102175
12. Lambiase F, Yanala PB, Pace F, Andreucci E, Paoletti A (2025) Thermal history and microstructural evolution in MIG-Wire Arc Additive Manufacturing of low carbon steel: influence of key process parameters. Int J Adv Manuf Technol 139:4125–4139
13. Lambiase F, Yanala PB, Paoletti A (2025) Thermal, microstructural, and mechanical characterization of early-stage deposition in wire arc additive manufacturing. Int J Adv Manuf Technol 138:953–970
14. Dirisu P, Ganguly S, Mehmanparast A, Martina F, Williams S (2019) Analysis of fracture toughness properties of wire+arc additive manufactured high strength low alloy structural steel components. Mater Sci Eng A 765:138285
15. Ge J, Lin J, Fu H, Lei Y, Xiao R (2018) Tailoring microstructural features of wire arc additive manufacturing 2Cr13 part via varying inter-layer dwelling time. Mater Lett 232:210–213
16. Liberini M, Allegretti G, Astarita A et al (2017) Selection of optimal process parameters for wire arc additive manufacturing. Procedia CIRP 62:470–474
17. Nagasai BP, Malarvizhi S, Balasubramanian V (2023) Effect of interlayer delay on microstructure and bead geometry of wire arc additive manufactured low carbon steel components. Int J Interact Des Manuf 17:939–946
18. Warsi R, Kazmi KH, Chandra M (2022) Mechanical properties of wire and arc additive manufactured component deposited by a CNC controlled GMAW. Mater Today Proc 56:2818–2825
19. Aldalur E, Veiga F, Suárez A, Bilbao J, Lamikiz A (2020) High deposition wire arc additive manufacturing of mild steel: Strategies and heat input effect on microstructure and mechanical properties. J Manuf Process 58:615–626
20. Ma C, Li C, Yan Y, Liu Y, Wu X, Li D, Han Y, Jin H, Zhang F (2021) Investigation of the in–situ gas cooling of carbon steel during wire and arc additive manufacturing. J Manuf Process 67:461–477
21. Hackenhaar W, Mazzaferro JAE, Montevecchi F, Campatelli G (2020) An experimental–numerical study of active cooling in wire arc additive manufacturing. J Manuf Process 52:58–65
22. Scotti A, Teixeira FR, da Silva LJ, de Araújo DB, Reis RP (2020) Thermal management in WAAM through the CMT Advanced process and an active cooling technique. J Manuf Process 57:23–35
23. Carvalho GHSFL, Campatelli G (2025) Control of interpass temperature and arc oscillation for improved mechanical properties and geometrical uniformity in Ti6Al4V alloy deposition using wire arc additive manufacturing. Int J Adv Manuf Technol 136:5025–5041
24. Suryakumar S, Karunakaran UCKP, Somashekara MA (2013) A study of the mechanical properties of objects built through welddeposition. Proc Inst Mech Eng Part B J Eng Manuf
25. Thien A, Saldana C, Kurfess T (2022) The effect of WAAM process parameters on process conditions and production metrics in the fabrication of single-pass multi-layer wall artifacts. Int J Adv Manuf Technol 119:531–547
26. Jorge VL, Teixeira FR, Scotti A (2022) Pyrometrical interlayer temperature measurement in WAAM of thin wall: strategies, limitations and functionality. Metals 12:765
27. Prado-Cerqueira JL, Camacho AM, Diéguez JL, Rodríguez-Prieto Á, Aragón AM, Lorenzo-Martín C, Yanguas-Gil Á (2018) Analysis of Favorable Process Conditions for the Manufacturing of Thin-Wall Pieces of Mild Steel Obtained by Wire and Arc Additive Manufacturing (WAAM). Materials 11:1449
28. Teixeira FR, Scotti FM, Jorge VL, Scotti A (2023) Combined effect of the interlayer temperature with travel speed on features of thin wall WAAM under two cooling approaches. Int J Adv Manuf Technol 126:273–289

Publisher's note Springer Nature remains neutral with regard to jurisdictional claims in published maps and institutional affiliations.